

# **Bi<sub>0.99</sub>Sb<sub>0.01</sub> Thin Film Transport Properties and Size Effect**

**M.A.M. Seyam**

*Department of Physics, Faculty of Education, Ain Shams University  
Roxy, Cairo, Egypt  
E-mail: [Seyam80@yahoo.com](mailto:Seyam80@yahoo.com)*

*Bi<sub>0.99</sub>Sb<sub>0.01</sub> thin films were vacuum deposited on glass substrates at room temperature. X-ray structural studies were performed. The thickness dependence of both the dc electrical resistivity and the Hall coefficient were carried out at room temperature over a thickness range from 30 nm to 200 nm. The type of conduction, the concentration and the mobility of charge carriers were revealed. Analysis incorporating the electrical resistivity and the Hall effect data led to the determination of the specular and non-specular size-effect parameters. Parameters such as the bulk resistivity ( $r_o$ ), bulk mean free path ( $l_o$ ), grain-boundary transmission coefficient ( $p$ ), external surface parameters ( $U$ ), surface scattering factor ( $p$ ) and grain-boundary parameter ( $V$ ) were all evaluated without using any adjusting parameters. Beside the background contribution to the film resistivity, an estimation of the contribution of the surface and grain boundary to the film resistivity were also carried out.*

## **1. Introduction**

Bi and Sb are typical semimetals materials, in which an overlapping between the conduction band and the valence band occurs [1]. Meanwhile, alloys of Bi and Sb, over certain composition range, are semiconductors with a narrow band gap [2,3] and the forbidden band width does not exceed 30meV.

The transition from semimetal to semiconductor state for Bi-Sb alloys depends upon many factors, the most important of which are the antimony concentration, the doping materials, the magnetic field, the technique and method of preparation [4,5].

Bi-Sb has received considerable attention since it has unique properties of the current carriers [3]. It has small thermal heat capacity, many- valley nature of the energy-spectrum of the current carriers, the high mobility and the resistivity of Bi-Sb thin films shows a small temperature dependence between liquid

nitrogen and room temperature [3,5]. Bi-Sb is an efficient thermoelectric material at low temperature [3,4,6]. The constituents of  $\text{Bi}_{0.99}\text{Sb}_{0.01}$  thin films have been the subject of many studies since it is regarded as one of the constituent materials of many binary and ternary compounds used in electronic devices. Previous studies [7-12] revealed that Bi-Sb thin film form crystallized in the hexagonal system and they also found that, the mean grain size increased with increasing the film thickness and decreased with Sb content. Many studies [7,12-16] revealed that with decreasing film thickness, the resistance increases regularly, though as the thickness reaches certain magnitude,  $\rho$  starts to drop manifesting an anomalous size effect.

However, the resistance of thinner film increases with temperature. This is due to a rapid decrease of the mean free path with temperature when it is less than the grain size and grain boundary blocking of conduction electrons occurs. The grain boundary barrier activation energy decreases with increasing thickness. Semi-conducting behaviour in thin film of Bi-Sb alloys had observed as reported in [14,15] while, in the bulk alloy of this composition shows a metallic behaviour. The carrier mobility and concentration were calculated from the electrical conductivity and low field Hall effect and magneto-resistance.

The classical size effect may be recognized as long as the film thickness is comparable with the carrier mean free path [17]. Since the mean free path is limited by surface and grain-boundary scattering, the transport properties of thin films may manifest such as effect.

Albeit the thickness dependence of the transport properties of thin films has been intensively investigated, the size-effect parameters were enormously inconsistent [17-19]. Such inconsistency may be ascribed to the film structure, preparation technique and the applied model and utilized approximation.

The size-effect parameters were determined employing size-effect theories of Fuchs, Sondheimer and Mayadas and Shatzkes as reported in [20]. The thermoelectric-power and electrical resistivity data were analyzed to determine the size-effect parameters [18] employing the mean-free-path theory of the size effect [20-23]. Despite the fair amount of work concerning the determination of the size-effect parameters of  $\text{Bi}_{0.99}\text{Sb}_{0.01}$  thin films, the results unveil wide discrepancies.

The aim of this study is to measure the electrical resistivity simultaneously with the Hall coefficient, in order to analyze the data and to reveal the size-effect parameters without using any adjusting parameters. In addition, it aims to anticipate the contribution of the background, surface and grain-boundary scattering to the thin-boundary resistivity.

## 2. Experimental Detail

Thin films of  $\text{Bi}_{0.99}\text{Sb}_{0.01}$  were thermally evaporated onto clean glass substrates under vacuum ( $10^{-6}$ Torr). The substrate temperature was held constant at room temperature. A  $9 \text{ nm s}^{-1}$  rate of deposition was attained in all deposited films. The film thickness was controlled by a quartz-crystal monitor and then precisely detected using the multiple-beam Fizeau fringes method [24]. Simultaneous measurements of Hall coefficient and dc resistivity, films of typical Hall-effect shape with four leads, two for the Hall voltage and two for the surface resistivity measurements, were prepared. The structural investigation carried using X-ray.

A dc technique was employed to measure the Hall coefficient at room temperature. A potentiometer with  $0.05 \mu\text{V}$  accuracy was used as detector. In the same measurement the magnetic field was switched off and the surface resistivity was potentiometrically measured using the same potentiometer.

## 3. Results and Discussion

### 2.1. Structural Characterization of $\text{Bi}_{0.99}\text{Sb}_{0.01}$ thin films:

X-ray diffraction patterns of  $\text{Bi}_{0.99}\text{Sb}_{0.01}$  thin films were obtained. A typical X-ray diffraction pattern of  $\text{Bi}_{0.99}\text{Sb}_{0.01}$  thin films in comparison to the powder of the same samples is depicted in Fig. (1). The patterns show that the film exhibits a polycrystalline structure with the (003) plane as preferred orientation rather than the (102) plane of powder form. Regarding Fig.(1), the  $\text{Bi}_{0.99}\text{Sb}_{0.01}$  thin films have a hexagonal crystal structure with the lattice parameters  $a=4.53\text{\AA}$  and  $c=11.81 \text{\AA}$ . The electron diffraction pattern for  $\text{Bi}_{0.99}\text{Sb}_{0.01}$  thin films are also given in the Fig.1. The analysis of this electron diffractogram showed that  $\text{Bi}_{0.99}\text{Sb}_{0.01}$  thin film has a polycrystalline nature of hexagonal phase. The calculated d-spacing of (hkl) lines observed from the X-ray technique and the electron diffraction pattern (Table 1) showed that the  $\text{Bi}_{0.99}\text{Sb}_{0.01}$  thin film has a polycrystalline nature of hexagonal phase which is agreement with previous data[7].

### 2.2. DC Electrical Resistivity ( $\rho$ ) of $\text{Bi}_{0.99}\text{Sb}_{0.01}$ thin films

The electrical surface resistivity was measured at room temperature(300K) for  $\text{Bi}_{0.99}\text{Sb}_{0.01}$  thin films. A typical size effect tendency was observed for the variation of  $\rho$  against the film thickness, as shown in Fig. (2). It is clearly seen that, for small thicknesses, the film resistivity thickness depends while at relatively large it is not. Such a trend can be attributed to the scattering sources associated with the film structure. This will be discussed in more detail later.

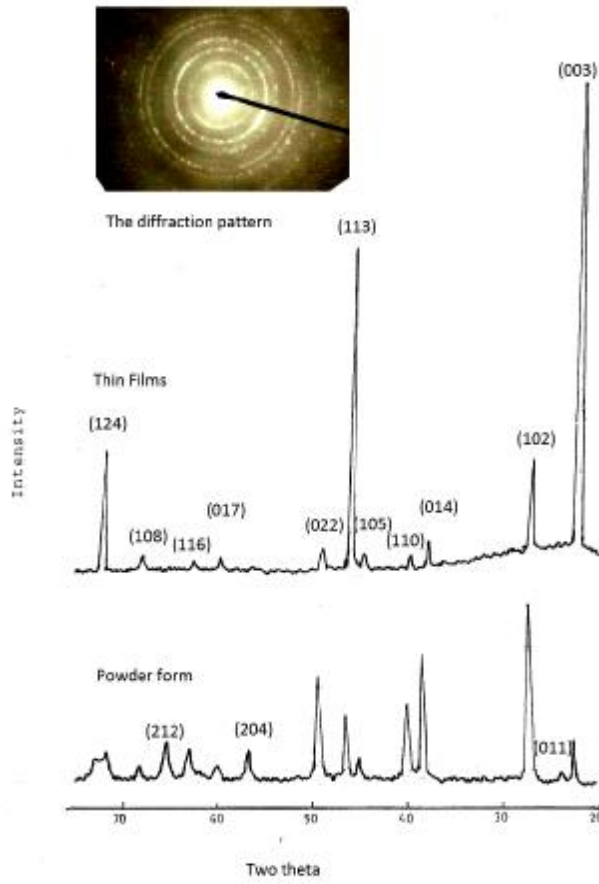


Fig.(1): X-ray and electron diffraction pattern

Table (1): Electron microscope analysis of Bi<sub>0.99</sub>Sb<sub>0.01</sub> thin films together with X-ray analysis

From electron microscope		From X-ray analysis		(hkl)
r(cm)	d(A)	powder d(A)	Thin film d(A)	
0.760	5.874	-	-	(002)
1.141	3.912	3.912	3.924	(003)
1.369	3.261	3.263	3.264	(102)
1.369	3.261	3.263	3.264	(102)
1.9	2.350	2.354	2.350	(014)
1.974	2.261	2.363	2.176	(110)
2.467	1.810	1.850	1.855	(022)
2.748	1.624	1.625	1.635	(204)

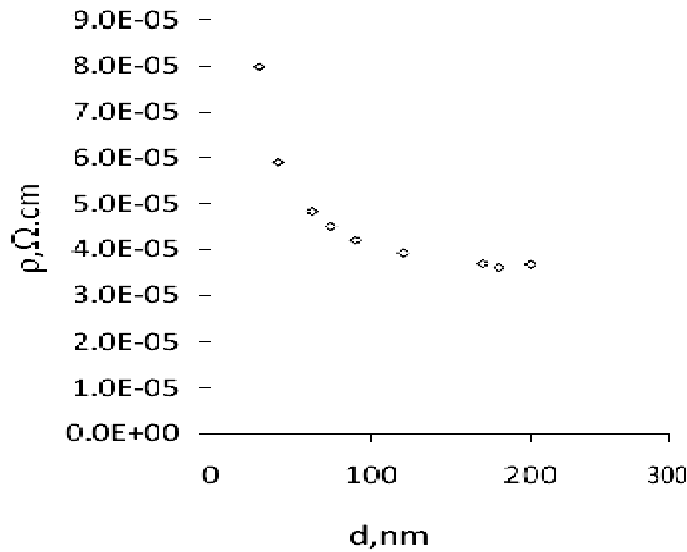


Fig.(2): Thickness dependence of the dc resistivity for Bi<sub>0.99</sub>Sb<sub>0.01</sub> thin films.

**2.3. Hall Coefficient of Bi<sub>0.99</sub>Sb<sub>0.01</sub> thin films (R<sub>h</sub>)**

The low field (0.781T) Hall coefficient of Bi<sub>0.99</sub>Sb<sub>0.01</sub> thin films was measured at room temperature against the film thickness. The Hall coefficient of Bi<sub>0.99</sub>Sb<sub>0.01</sub> thin films, over the thickness range between 30 nm to 200 nm, at room temperature was found to have a positive value which is agreement with the previously reported data from Hall coefficient and thermoelectric power measurements [18].

As shown in Fig.(3), Hall coefficient seems to decrease with increasing film thickness. The positive sign of the Hall coefficient of Bi<sub>0.99</sub>Sb<sub>0.01</sub> thin films can be attributed to the presence of localized states near the band edges. Considering that one type of charge carriers is dominating, the concentration of the charge carriers (n) was calculated using

$$R_h = 1/ne \tag{1}$$

where e is the electronic charge and R<sub>h</sub> is the Hall coefficient. The concentration of charge carriers (n) was calculated for Bi<sub>0.99</sub>Sb<sub>0.01</sub> thin films at room temperature and found to have values 1.87-2.08x10<sup>19</sup>cm<sup>-3</sup>. The reported value[18] of n is in reasonable agreement with our calculated value at room temperature. The Hall mobility, μ was calculated according to

$$\mu = R_h / \rho \tag{2}$$

The estimated average value of  $\mu$  is  $6.901 \times 10^3 \text{ cm}^2/\text{Vs}$ . For calculating the Fermi energy  $E_f$ , the following equation is employed [18];

$$E_f = (\hbar^2/2m^*) (3n/8\pi)^{2/3} \tag{3}$$

where  $\hbar$  is Planck's constant,  $m^*$  is the effective mass was substituted by the rest electron mass [18]. The calculated average value of  $E_f$  at room temperature equals 0.046 eV. Also For small thicknesses, the Hall mobility,  $\mu$  and the Fermi energy  $E_f$  depends on the thickness while at relatively large thickness they are not as shown in Fig.(4,5).

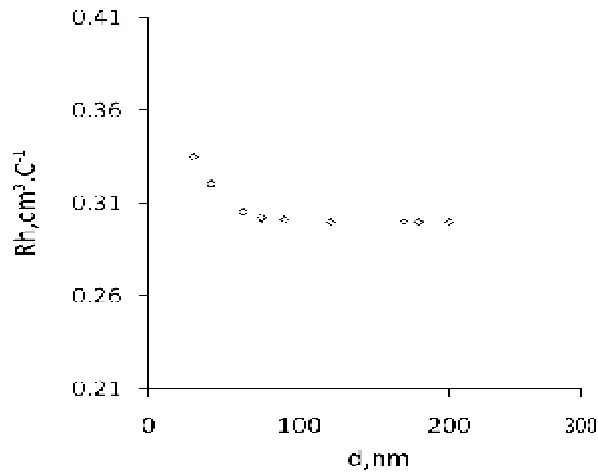


Fig.(3): Variation of Hall coefficient,  $R_h$  vs film thickness of  $\text{Bi}_{0.99}\text{Sb}_{0.01}$  thin films.

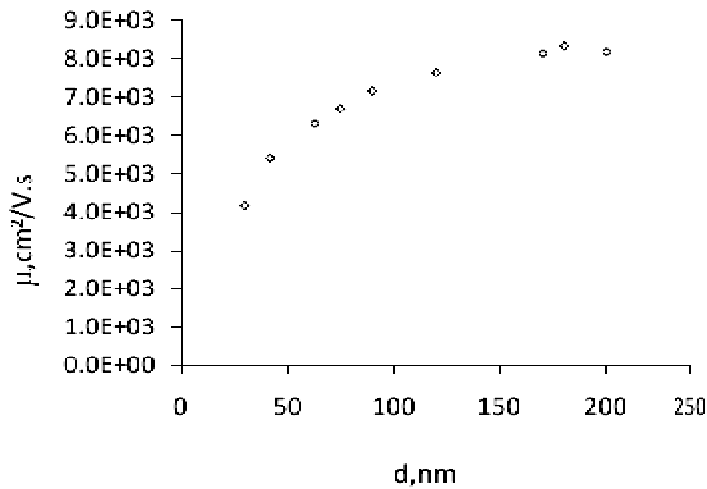


Fig.(4): Thickness dependence of Hall mobility ( $\mu$ ) for  $\text{Bi}_{0.99}\text{Sb}_{0.01}$  thin films.

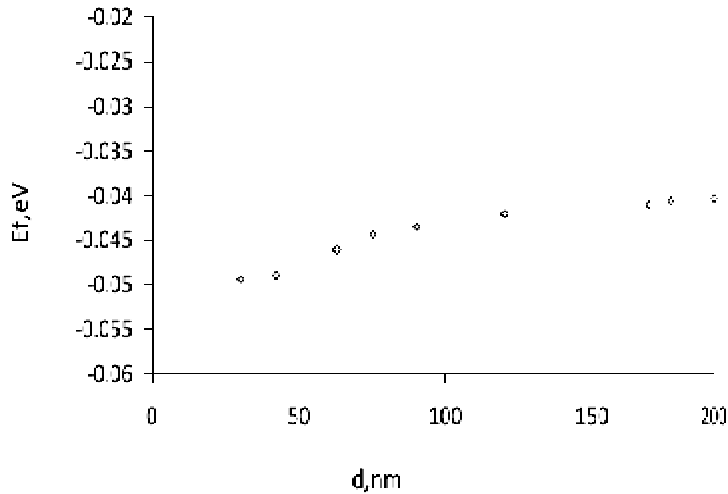


Fig.(5): Thickness dependence of  $E_f$  for  $\text{Bi}_{0.99}\text{Sb}_{0.01}$  thin films.

#### 2.4. Size effect parameters of $\text{Bi}_{0.99}\text{Sb}_{0.01}$ thin films

A great deal of work, both experimentally and theoretically, has been devoted to the study of size effects in thin films [19,25]. In order to find out the size-effect parameters, a simple analytical expression, derived by Teller [25], for the electrical resistivity,  $\rho$  in terms of film thickness,  $d$  is introduced as:

$$\rho d = \rho_0 d + 3\rho_0 \lambda_0 (1-p)/8 \quad (4)$$

where  $\rho_0$ ,  $p$  and  $\lambda_0$  are the resistivity of a thick film, the surface scattering factor and the charge carrier mean free path in a thick film respectively. From equation (4), it is evident that the relationship between the multiple  $\rho d$  and the film thickness  $d$  is linear. The slope of such a relationship yields the so-called bulk resistivity ( $\rho_0$ ). Furthermore, the bulk mean free path ( $\lambda_0$ ) can be calculated by means of the intercept of the obtained straight line with the  $\rho d$  axes.

Fig.(6) represents the experimental size-effect plot between  $\rho d$  and  $d$  at room temperature, where, according to equation (4), a straight line is displayed. The slope of the line yields  $\rho_0 = 29.43 \mu\Omega\text{cm}$ . This value agrees rather well with previously reported values, as indicated in Table (1). In order to calculate the bulk mean free path ( $\lambda_0$ ), two procedures can be followed.

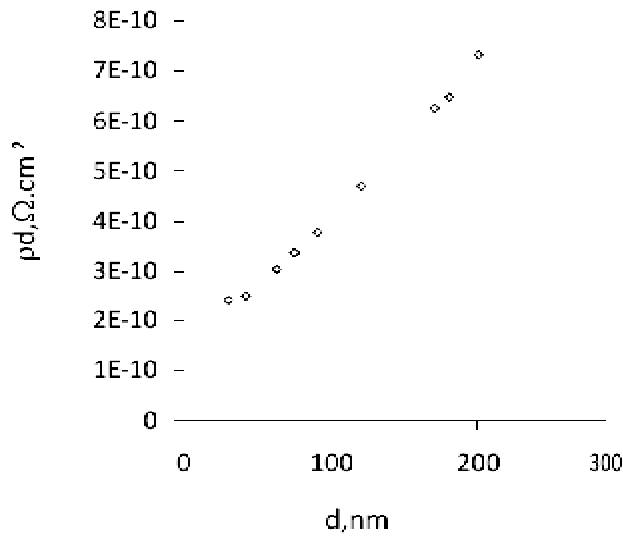


Fig.(6): Size effect plot between ρd vs d for Bi<sub>0.99</sub>Sb<sub>0.01</sub> thin films.

**2.4.1. Non-Specular Scattering**

Regarding surface scattering [19,25], the specular parameter P takes on values between 0 and 1. In non-specular scattering, where surface scattering is assumed to be completely diffusive, p is presumed to be 0. Accordingly, equation (4) is rewritten as

$$\rho d = \rho_0 d + 3\rho_0 \lambda_{on} / 8 \tag{5}$$

where  $\lambda_{on}$  is called bulk mean free path for the non-specular scattering. Equation (5) represents a straight line between ρd against the film thickness d, the intercept of which with the coordinate renders the bulk mean free path for non-specular scattering ( $\lambda_{on}$ ). From Fig.(6), was found to be 11.4 μm. A reasonable agreement was found between this value and the published ones see Table (2).

**Table (2):** Size-effect parameters of Bi<sub>0.99</sub>Sb<sub>0.01</sub> thin films

ρ <sub>0</sub> , μΩcm	λ <sub>on</sub> , μcm	λ <sub>os</sub> , μcm	P	P-	U	V
29.43	11.4	58.1	0.80	0.968	0.832	2.842



### 2.4.2. Specular Scattering

For the more general case of partial diffuse scattering of charge carriers on the external surface,  $p$  has values in the range  $0 < p < 1$ . Many techniques frequently rely on adjusting parameters [17, 19, 26, 27].

The thermoelectric power and the electrical resistivity data were analyzed together for the determination of size-effect parameters [18]. In this study, the Hall effect, instead, is analyzed with the dc resistivity data to figure out the size-effect parameters without utilizing any adjusting parameters. The resistivity's mean free path,  $\lambda_{os}$  and number of charge carriers,  $n$  are related according to relation [18].

$$\rho_o \lambda_{os} = (h/2e^2) (\pi n^2/3)^{-1/3} \quad (6)$$

From the Hall-effect data, the concentration of charge carriers  $n$  can be substituted. Consequently,  $\rho_o \lambda_{os}$  was estimated and found to be  $1.71 \times 10^{-9} \Omega \text{cm}^2$ . The specular parameter  $p$  from equation (4) can now be easily obtained and is found to be 0.8, as listed in Table 2, it agrees rather well with the value of [17].

Since  $\rho_o$  was calculated before (slope of Fig.6) regarding equation (6), the value of the bulk mean free path of the specular case  $\lambda_{os}$  was worked out. The value of  $\lambda_{os}$  equals  $58.1 \mu\text{m}$  which (Table 2) is in rather good agreement with results of [17]. For polycrystalline films, in accord with Mattheissen's rule and the independent mean free path model, the total film resistivity  $\rho$  is assumed to be due the contribution of three types of scattering [17,19,26,27]. These simultaneously operating types are: the back ground (bulk), surface and the grain-boundary scattering. Therefore,

$$\rho = \rho_o + \rho_s + \rho_g \quad (7)$$

where  $\rho_s$ ,  $\rho_g$  refer to the resistivity associated with the surface and grain-boundary scattering, respectively. A simple formula follows for the surface-scattering contribution to the thin-film resistivity [17];

$$\rho_s = 3\rho_o \lambda_{os} (1-p)/8d \quad (8)$$

Using our results of Table 1 and equation (8),  $\rho_s$  was calculated for each thickness. It has been found that  $\rho_s$  is significantly thickness-dependent. The thickness dependence of  $\rho_s$  is shown in Fig.(7).

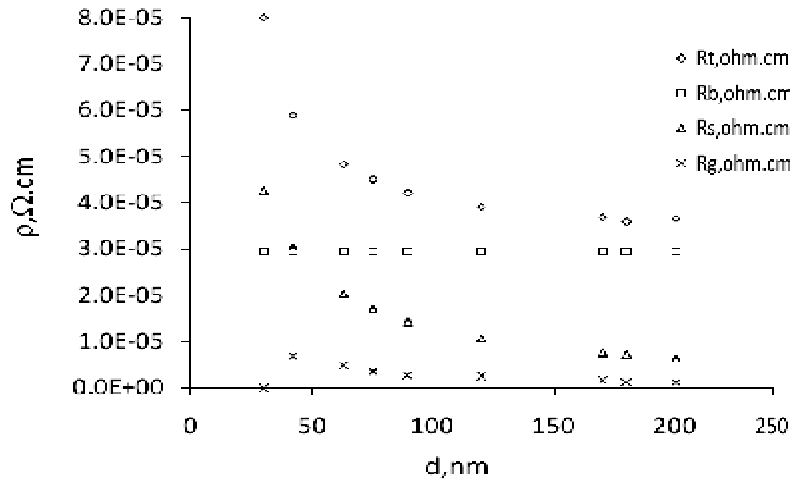


Fig.(7): Thickness dependence of  $\rho$ ,  $\rho_o$ ,  $\rho_s$  and  $\rho_g$  of  $Bi_{0.99}Sb_{0.01}$  thin films.

Equation (7) can now be applied to deduce the contribution of the grain-boundary scattering  $\rho_g$  the grain-boundary resistivity was also found to be thickness-dependent. The variation of  $\rho_g$  against film thickness is depicted in Fig.(7). A few things can be deduced from Fig. (7). Firstly,  $\rho_s$  is as effective as  $\rho_o$ , especially at low thickness. Secondly, the effect of  $\rho_g$  is considerable and cannot be neglected at low thickness. Thirdly, the background scattering dominates the film resistivity in the higher thickness range.

A similar expression can be assumed for  $\rho_g$  as follows :

$$\rho_g = 3\rho_o\lambda_{os}(1 - p^-)/8d \tag{9}$$

where  $p^-$  is another size effect parameter called transmission coefficient of carries, i.e., the fraction of carries which are specularly transmitted through the grain boundaries.

According to equation (9), the slope of  $\rho_g$  against the reciprocal of film thickness, depicted in Fig. (8), enables the evolution of parameter  $p^-$ .

Table 1 includes the obtained value of  $p^-$  in comparison with available data, where a quite good agreement is found with [17].

Other size –effect parameters [22], such as the external surface parameter (U) and the grain-boundary parameter (V) were determined according to:

$$U = (d/\lambda_{os})[\ln(1/p)] \quad (10)$$

and

$$V = (D/\lambda_{os})[\ln(1/p)] \quad (11)$$

where D is the grain diameter that it determined from x-ray ( $D=87.31$  nm and  $d=120$  nm). U and V were calculated and are listed in Table (2) with the other available data for comparison.

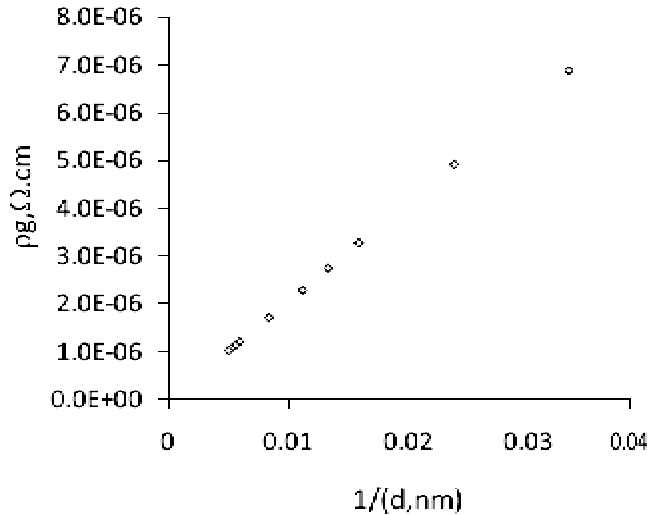


Fig.(8): Plot of the variation of  $\rho_g$  for  $\text{Bi}_{0.99}\text{Sb}_{0.01}$  thin films.

### 3. Conclusions

It has been revealed from the X-ray investigation that deposited  $\text{Bi}_{0.99}\text{Sb}_{0.01}$  thin films were polycrystalline films of hexagonal crystal structure with  $a=4.53\text{\AA}$  and  $c=11.81\text{\AA}$ .

It has been found that the thickness dependence of resistivity exhibits a size effect. The Hall effect measurements showed that  $\text{Bi}_{0.99}\text{Sb}_{0.01}$  thin films behave as a p-type semiconductor with a concentration of hole carriers of  $2.04 \times 10^{19} \text{ cm}^{-3}$ . The Fermi energy and Hall mobility were found to be  $0.046 \text{ eV}$  and  $6.901 \times 10^3 \text{ cm}^2/\text{Vs}$ , respectively. Without using neither adjusting parameters nor fitting techniques, the size-effect parameters were concluded directly from the experimental data of resistivity in conjunction with the Hall-effect data.

In addition to the background resistivity, the resistivity due to the contribution of the surface and grain-boundary scattering were deduced from the total film resistivity. It was concluded that the surface and the grain-boundary scattering are significantly effective at low thicknesses.

The author acknowledge the help of Prof. A.ElFalaky, Physics department, Faculty of Science, Zagazig University for his support and help throughout this work.

## References

1. V.D. Das and N.Soundararajan, *J.Mater. Sci.*, **24**, 4315 (1989).
2. F.Volklein and E.Kessler, *Phys.Sol.stat. b*, **134**, 351(1986).
3. O.S.Gryanov, G.A.Ivanov, B.Ya. Moizhers, V.N. Naumov, Z.A. Nemchinskif, N.A.Rodinov and N.A.Redko, *Sov. Phys. Sol. stat.*, **24**, 1326 (1982).
4. F.Volklein and E.Kessler, *Thin Solid Films*, **155**, 197 (1987).
5. S.Takabe and H.Oono,*Thin Solid Films*, **145**, 171 (1986).
6. V.D. Das and N. Meena, *Phys. stat. sol. B*, **104**, k89 (1981).
7. R.Tolutis, V.Tolutis, J.Novickij and S.Balevicius, *Semicond. Sci. Technol.* **18**, 430, (2003)
8. F.Volklein and E.Kessier, *Thin Solid Films*, **155**, 197 (1987).
9. M.Hashimoto, *Thin Solid Films*, **130**, 171(1985).
10. S.Takabe and Osono, *Thin Solid Films*, **145**, 171 (1986).
11. J.Buxo, M.Saleh, G.Sarrabayrouse, G.Dorville, J. Berty and M. Brieu, *Rev. Phys. Appl.*, **15**, 961 (1980).
12. F.Volklein and E.Kessier, *Phys. Stat. Sol.*, (b) **134**, 351 (1986).
13. F.Volklein and E.Kessier, *Phys. Stat. Sol.*, (b) **143**, 121 (1987).
14. V.D.Das and N.Meena, *Phys. Stat. Sol.*, B, **104**, K89 (1981).
15. Y.F. Komink, E.I. Bukhshtab and Y.V. Nikitin, *J. De phys.*, **39**, 142 (1978).
16. F.Volklein and U.Dillner, *phys. stat. sol.*, (b) **162**, 147 (1990).
17. A. Kumar, O.P. Katyal: *J. Mater. Sci.*, **24**, 4037 (1989).
18. V.D. Das, N. Soundararajan: *J. Mater. Sci.*, **24**, 4315 (1989).
19. D. Deschacht, A. Boyer: *J. Mater. Sci. Lett.*, **4**, 25 (1985).
20. C.I. Wu, S.N.Girard, J.Sootsman, E.Timm, E.D.Case, M.G. Kanatzidis, H.Schock, D.Y.Chung and T.P.Hogan, *Materials Research Society*, **1314**, 10 (2011)
21. D. Deschacht, A. Boyer: *J. Mater. Sci.* **20**, 807 (1985).
22. A.F. Mayadas, M. Shatzkes: *Phys. Rev.*, **B1**, 1382 (1970)
23. C.R. Teller, A.J. Tosser: *Thin Solid Films*, **70**, 225 (1980).
24. S.Tolansky "Multiple-bem" Interferometry of Surfacees and Films, London, Oxford, 147 (1988).
25. C.R. Teller: *Thin Solid Films*, **51**, 311 (1978).
26. C.R. Pichard, C.R. Teller, A.J. Tosser: *J. Mater. Sci.*, **15**, 2236 (1980).
27. C.R. Pichard, C.R.Teller, A.J. Tosser: *Phys. Status Solidi*, (a) **65**, 327 (1981).